

Article

Microfluidic Platform for Enzyme-Linked and Magnetic Particle-Based Immunoassay

Nikhil Bhalla ¹, Danny Wen Yaw Chung ^{1,*}, Yaw-Jen Chang ², Kimberly Jane S. Uy ¹, Yi Ying Ye ¹, Ting-Yu Chin ³, Hao Chun Yang ¹ and Dorota G. Pijanowska ⁴

¹ Department of Electronic Engineering, Chung Yuan Christian University, Zhongli 32023, Taiwan; E-Mails: nikhilbhalla151@gmail.com (N.B.); kimuy_1984@yahoo.com (K.J.S.U.); polnna25@gmail.com (Y.Y.Y.); derry2010@hotmail.com (H.C.Y.)

² Department of Mechanical Engineering, Chung Yuan Christian University, Zhongli 32023, Taiwan; E-Mail: justin@cycu.edu.tw

³ Department of Biotechnology, Chung Yuan Christian University, Zhongli 32023, Taiwan; E-Mail: tychin@cycu.edu.tw

⁴ Insititute of Biocybernetics and Biomedical Engineering, Polish Academy of Sciences, Warsaw 02-109, Poland; E-Mail: dpijanowska@ibib.waw.pl

* Author to whom correspondence should be addressed; E-Mail: wenyaw12@yahoo.com.tw; Tel.: +886-3-265-4615; Fax: +886-3-265-4699.

Received: 12 March 2013; in revised form: 4 June 2013 / Accepted: 4 June 2013 /

Published: 18 June 2013

Abstract: This article presents design and testing of a microfluidic platform for immunoassay. The method is based on sandwiched ELISA, whereby the primary antibody is immobilized on nitrocellulose and, subsequently, magnetic beads are used as a label to detect the analyte. The chip takes approximately 2 h and 15 min to complete the assay. A Hall Effect sensor using 0.35- μ m BioMEMS TSMC technology (Taiwan Semiconductor Manufacturing Company Bio-Micro-Electro-Mechanical Systems) was fabricated to sense the magnetic field from the beads. Furthermore, florescence detection and absorbance measurements from the chip demonstrate successful immunoassay on the chip. In addition, investigation also covers the Hall Effect simulations, mechanical modeling of the bead–protein complex, testing of the microfluidic platform with magnetic beads averaging 10 nm, and measurements with an inductor-based system.

Keywords: microfluidics; magnetic bead; immunoassay; Hall Effect; Bio-MEMS; bead–protein complex

1. Introduction

Microfluidic-based analyzers are currently receiving considerable attention in many clinical, diagnostic and pharmaceutical settings [1]. These systems have many potential advantages, including reduced reagent consumption, smaller analysis volumes, faster analysis time, higher levels of throughput and automation, and increased instrument portability [2–4]. These advantages provide highly efficient immunoassay platforms based on microfluidics. Most of the microfluidic technologies utilize closed channels permanently formed in glass, plastic or silicon, through which continuous flows of liquid are pumped by mechanical or electrokinetic means [2,5].

Among various solid-phase immunoassay formats in current use, the sandwich enzyme-linked immunoassay (ELISA) typically carried out in a polystyrene microtiter plates is superior to other types of heterogeneous solid-phase immunoassay with respect to sensitivity, specificity and kinetics [6,7]. This is due to the selectivity of antibody–antigen complex reactions, the use of excess capture antibody and enzyme–antibody conjugate, and the chemical amplification with enzyme conjugates that allows the detection of very low concentrations of analytes [8,9]. However, magnetic effect-based biomolecule detection is under rapid development due to its ability to detect single particles [10–12]. It has numerous advantages, such as its ease of use, portability, high sensitivity, and faster read-out technique [13]. Among the various kinds of magnetic effect-based biosensors are SQUID (superconducting quantum interference device), GMR (giant magneto resistor) [12,14,15], resonant coils, Micro-Electro-Mechanical Systems (MEMS)-based micro-cantilever and Hall effect-based devices. Most of these mechanisms are well suited for solid-phase assay involving simple to complex circuits. SQUID sensors have high sensitivity and low noise but are not compact and the temperature requirements of the superconducting makes them infeasible for biosensor applications. Materials used to fabricate GMR are infrequently used in the electronics industry [16,17]. Hall effect-based sensors, on the other hand, involve integrated circuit fabrication technology, analyte multiplexing and the capability of being fabricated as an array [9,10].

Previously magnetic beads have been used as immobilization surface for various components of complex biological reactions on microfluidic chips [18–22]; however, their use as a label has been explored in many studies. Use of magnetic beads as a label for immunoassays is, indeed, better as it avoids reaction with various chemical tags, which further reduces the assay time and increases sensitivity of the measurement system. Here, we successfully demonstrate ELISA on the designed microfluidic platform and its capability to successfully perform magnetic particle-based immunoassay, whereby the magnetic particles act as a label. We also proposed integration of highly sensitive and customized Hall sensor to sense the magnetic field, which is directly proportional to the analyte in the measurement.

2. Experimental Section

2.1. Materials and Immunoassay Protocol

The main objective is to develop a chip that detects the level of obesity in humans. Adiponectin is a protein that is an indicator of increased fat metabolism in the bloodstream. When the body suffers from the complications of obesity (e.g., high risk of diabetes, high cholesterol, cardiac stroke, *etc.*), the

concentration of adiponectin in the blood decreases. Therefore, the amount of adiponectin directly indicates the level of obesity. 4 µg/mL adiponectin polyclonal antibodies (bought from *Abnova*) are dispensed in PBS (phosphate buffered saline, 10 mM; pH 7) and are transported to the reaction chamber of the chip where they are immobilized on nitrocellulose. This is followed by the addition of blocking buffer (BSA, bovine serum albumin, 5% in PBS) to block the non-specific sites on nitrocellulose. Subsequently, 1 µg/mL adiponectin suspended in PBS and 4 µg/mL of adiponectin monoclonal antibodies (bought from *BioVision*) are pumped to form an antibody–antigen–antibody sandwiched complex. Between each of the aforementioned steps, incubation for 30 min at room temperature (25 °C) and serial washing (using PBS) for 1 min are carried out. Finally, the presence of antigen (adiponectin) is identified by two methods, firstly using horseradish peroxidase (HRP), which gives a color change at a specific wavelength of light and, secondly, using polyclonal antibody-coated magnetic beads (10 nm average bought from Taiwan Advanced Nanotech Inc., Taoyuan, Taiwan), where its magnetic field is measured using inductor-based system and Hall sensor. The coating of magnetic beads was done by Taiwan Advanced Nanotech Inc. There is no active mixing of reagents involved. Every reagent transports independently from each reagent storage chamber and sequentially forms the whole bio-complex. Since the magnetic beads are coated with polyclonal antibodies it attaches to the secondary antibody of adiponectin. The integration of a secondary antibody with the coated antibody on the beads traps them and forms the bio-complex shown in Figure 1.

2.2. Bio-Complex Mechanical Modeling

Magnetic beads coated with anti-antibody are attached to the protein sandwiched complex to form magnetic particle bio-complex structure (Ab–Ag–Ab–Bead complex). This superparamagnetic bead complex is sensed by the Hall effect sensor. Figure 1 shown below illustrates the biological complex modeled as a mechanical structure. Analysis for the von Mises stress and displacement of the complex from its central axis was done using COMSOL 3.5a. This was done to make sure that the Ab–Ag–Ab complex remains intact when the magnetic bead is added to it since the weight of magnetic bead is 10^5 times more than the Ab–Ag–Ab–Bead complex to be detected. At this moment, the fluid is not moving. The antibodies have been immobilized on the nitrocellulose deposited on the chip, which captures the antigen (adiponectin), and, subsequently, the secondary antibodies and magnetic beads gets attached and form the Ab–Ag–Ab–Bead complex. Therefore, it is modeled as a static system. Table 1 shows the weight and dimensions of each entity in the complex, which was taken into account for analysis. Magnetic properties of the beads were taken from Taiwan Advanced Nanotech beads data sheet. The generalized expression of the force experienced by a magnetic bead when placed in the magnetic field is shown by Equation (1). The bead experiences this force when it is becoming magnetized.

$$F_{MAP}(r_0) = 2\pi\mu_0 K(\mu_0\mu)a^3 \nabla[H_{ext}(r_0)^2] \quad (1)$$

The above equation shows the magneto static force (F_{MAP}) on the magnetic bead when placed in a magnetic field as a function of its size (radius r_0), where K is the Clausius–Mossotti constant in terms of absolute (μ_0) and relative (μ) permeability of the magnetic bead material. “ a ” is the distance of the bead from the source of the magnetic field. H_{ext} is the induced external magnetic field on the bead.

Figure 1. Mechanical model of a superparamagnetic nanoparticle—protein complex.

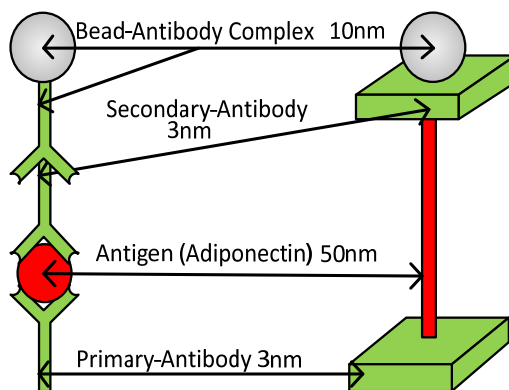


Table 1. Weight and dimensions of the each entity in the bio-complex.

	Average Weight (Kilograms)	Length (Angstroms)	Width (Angstroms)
<i>Adiponectin</i>	1.66×10^{-27}	500	8
<i>Antibody/Anti-Antibody</i>	6.64×10^{-23}	30	150
<i>Magnetic Bead</i>	10×10^{-18}	Average spherical diameter of 10 nm	

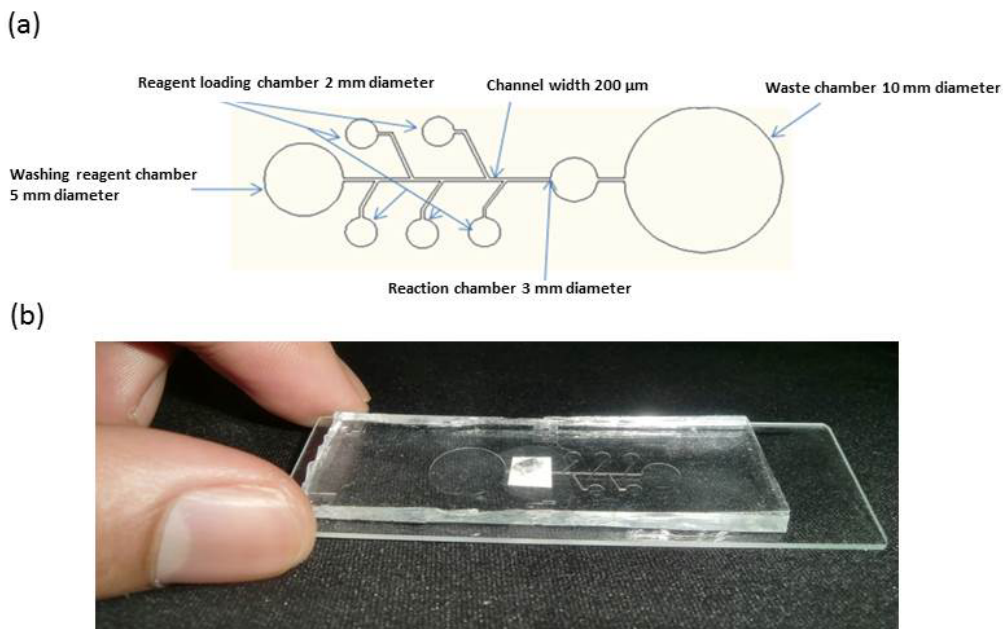
2.3. Fabrication of Microfluidic Platform

The design of the platform was made using AutoCAD-2010. Top view of the design is shown in Figure 2a. It has five reagent loading chambers (2-mm diameter), one reaction chamber (3-mm diameter), one washing reagent chamber (5-mm diameter) and one waste chamber (10-mm diameter).

A negative photo mask for the design was transferred on the SU-8 coated FR-4 wafer to form a mold which was transferred to poly-di-methyl-siloxane (PDMS). The formation of the mold starts with the washing of FR-4 wafer (printed circuit board) with acetone, methanol and distilled water. After the wafer was cleaned and dried by nitrogen gas, SU-8 was spin coated (Spin Coater: K3595D-1, Kyowariken) on the wafer for 30 s each at a speed of 500 rpm, 750 rpm and 1000 rpm. Then, the wafer was soft baked up to 7 h. The temperature was varied from 25 °C to 95 °C, using PID controlled heating oven (S.J. High Technology, Taipei City, Taiwan). Next, the wafer was exposed to ultraviolet light (UV-A365) and the mask was transferred using negative photolithography. This step was followed by baking from 25 °C to 65 °C. There was a rise of 1 °C for every minute and the wafer was baked for 30 min at 65 °C and held back for 40 min at 25 °C when the temperature is dropped from 65 °C. This process takes about 2 h. Finally using poly-glycol-methyl ether acetate (PGMEA) and 2-Propanol, a SU-8 mold was developed. At this stage, silicon elastomer A (Sylguard 184A), silicon elastomer B (Sylguard 184B) and silicon oil are mixed together in 10:1:1 ratio to form poly-di-methyl-siloxane (PDMS). This solution was poured on the SU-8 mold and, after 2 h of soft baking, the PDMS structure of the design is ready. This PDMS structure was then plasma bonded using plasma cleaner (Harrick Plasma, Ithaca, NY, USA) on a glass slide coated with a nitrocellulose membrane at the position of the reaction chamber. Nitrocellulose films and glass slides were dipped in a mixture of diethyl ether and ethanol (20% in aq.) for 30 s, after which the film was placed at the desired location

on the glass slide. It was then placed in 20% aq. solution of ethanol and left to dry overnight to harden. Figure 2b shows the final fabricated microfluidic platform.

Figure 2. (a) scheme for microfluidic platform design (b) fabricated microfluidic platform (white color depicts the nitrocellulose coating at the reaction chamber).



2.4. Hall Sensor Fabrication

The sensing platform designed using BioMEMS TSMC 0.35- μm technology has two parts: Hall sensor and induction coil. Figure 3 shows the layout of the design in Virtuoso on the Cadence environment. This is a 2P4M (2-poly 4-metal) process which involves passivation etching of the sensing area followed by RLS etch and gold deposition. A gold layer is used in this process to protect the underlying circuitry. In addition, the gold layer is also biocompatible and is inactive in liquid medium. The Hall sensing area is made up N-well, which has a thickness of 1.6 μm . The induction coils have a thickness of around 22.2 μm made from metal-2, meta-3 and meta-4 layers. The distance between induction coil and sensing area is 21.6 μm . The Hall’s sensing area is 10 $\mu\text{m} \times 10 \mu\text{m}$. The process steps of the fabrication are illustrated in Figure 4.

Figure 3. Layout of Hall sensor area (yellow) and induction coil (red).

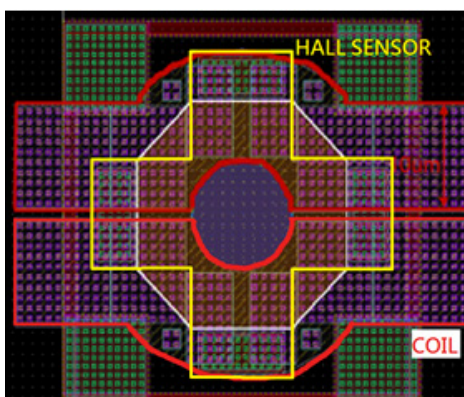
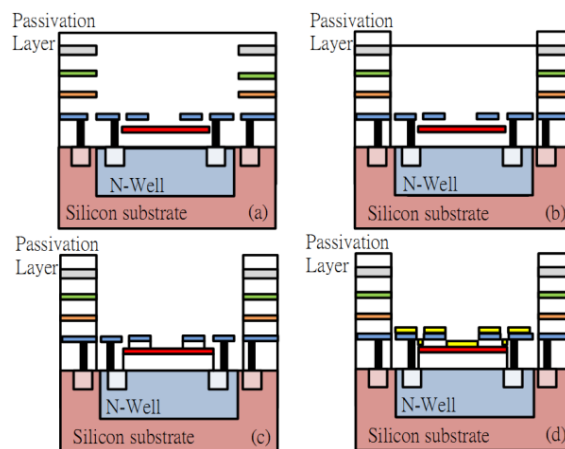


Figure 4. Fabrication process (a) after-standard TSMC 0.35- μm CMOS process (b) removal of passivation layer (c) RLS etch (d) gold coating.



The Hall sensor is based on the principle that the presence of an out-of-plane magnetic field causes the current in a conductor to be deflected. The deflection of current in a conductor causes a potential difference to build across the conductor [10,11]. The Hall voltage is given by Equation (2).

$$V_H = kI_b B \quad (2)$$

In the above Equation (2), V_H is the Hall's voltage, I_b is the input current and B is the magnetic field perpendicular to the direction of current. k denotes the sensitivity (current) of the Hall's platform. k is mathematically defined in terms of n (doping concentration = 1.5×10^{15}), q (electron charge = -1.6×10^{-19}) and d (N-well thickness = 1.6×10^{-6} μm). The value of k is calculated as -2.6×10^5 using Equation (3).

$$K = 1 / nqd \quad (3)$$

3. Results and Discussion

Designing the microfluidic platform involves following basic operations: pumping and transport of reagents to the reaction chamber; immobilization of antibodies, antigen and magnetic beads; and washing steps. First, the assay was confirmed by the secondary antibody conjugated to HRP whose activity was detected with a color-forming product. Then, the response from the magnetic beads was measured from the Hall effect sensor and inductor-based system. The Hall sensor is fabricated to measure a very small amount of the magnetic field from (in range of milli-Tesla) nano-sized superparamagnetic beads. The Hall sensor structure also involves an inductor coil above the Hall sensing surface. The function of this inductor coil is to polarize the superparamagnetic beads and to interact with magnetic field from the bead. The interaction between the field from the nano beads and the coil increases the net magnetic field over the Hall sensing area. This change in magnetic field over the Hall surface identifies the magnetic bead, which indeed confirms the presence of protein. The second system *i.e.*, inductor-based system (fabrication is cost efficient) was also made to detect the magnetic field.

The results shown in Figures 5 and 6 confirm that the whole structure does not buckle. Folding of the proteins forms a cushioned structure, which is good enough to hold the magnetic bead, of weight

10^5 times heavier than the biological complex. Slight bending is observed in the complex. The main body of the magnetic bead is made up of polystyrene, which contains large number of magnetic nanoparticles. In magnetic particles of such a small size, all atomic magnetic moments are aligned, but the direction of this total magnetic moment can rotate freely under the influence of thermal fluctuations at room temperature [23].

Figure 5. Total deformation of the bio-complex.

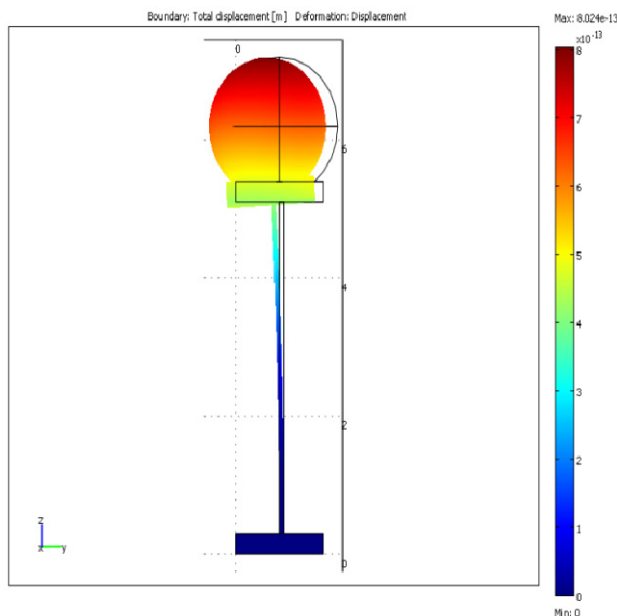
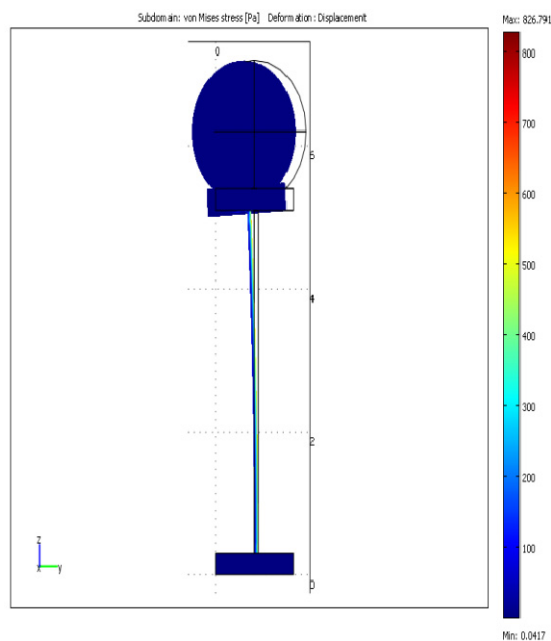
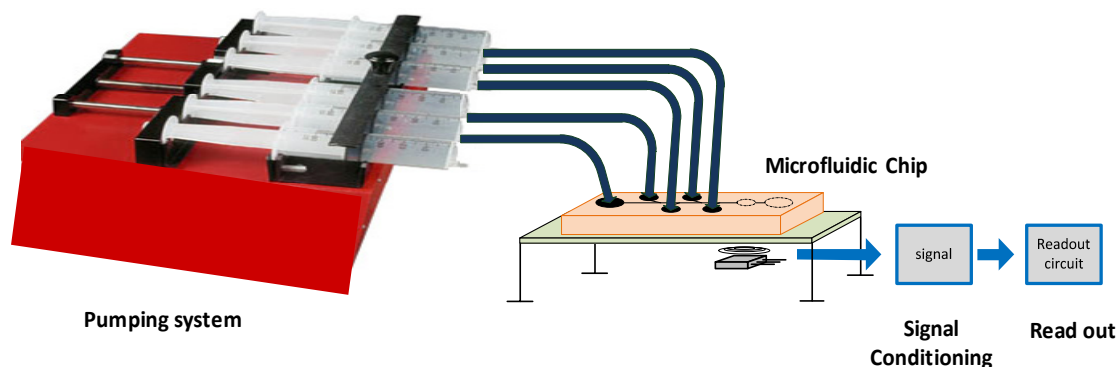


Figure 6. Von Mises stress distribution plot of bio-complex.



The pumping/transport of fluid was carried automatically by a microcontroller-based programmed syringe pump system (Figure 7). The speed with which the fluid was moved was manipulated in terms of velocity of fluid at the outlet of pump. The average velocity of the fluid inside the microchannel was 1 mm/s. The reagent loading chambers were loaded with 3 μ L of all reagents.

Figure 7. Testing platform with pump and sensor to perform immunoassay.



To investigate the performance of the chip, the immunoassay was carried out as per the steps mentioned in the above protocol. HRP was added to the bio-complex and fluorescence was observed under spectrometer (Figure 8). Red light (wavelength = 750 nm) was passed through the whole microfluidic device. On observing the image captured during spectrometric scan (Figure 8), we saw that the reaction was successfully completed at the reaction chamber. The wavelength of the fluorescent light at which maximum absorbance is observed from the reaction chamber is between 500–550 nm (Figure 8). At this wavelength, the fluorescence was observed using image analyses tool (image J), whereby the integrated fluorescence intensity (average $n = 30$) was observed around 55.7 a.u. These values were corrected by subtracting the background fluorescence to yield a corrected total fluorescence value of 47 a.u (Figure 9) (average for $n = 30$ chips). Figure 10 shows a comparative data of fluorescence detection on the chip and its controls. The absorbance with the analyte (adiponectin) was observed to be 2.8 times higher (0.37) than the control with maximum absorbance. To evaluate the significance of the data, Tukey’s multiple comparison test was performed. The test data revealed a significant difference between the immunoassay and its controls at significance level of 0.05 ($p < 0.05$). The mean difference between controls and immunoreaction was 0.236 to 0.288 in 95% confidence interval. Control reaction without the use HRP-linked antibody showed the least amount of absorbance value (0.08). However, a bit higher absorbance (0.11–0.13) was observed in other controls, owing to the fact that HRP-conjugated antibodies are much larger than other components of bio-complex and binds non-specifically to the nitrocellulose.

Figure 8. Fluorescent intensity on nitrocellulose vs. wavelength.

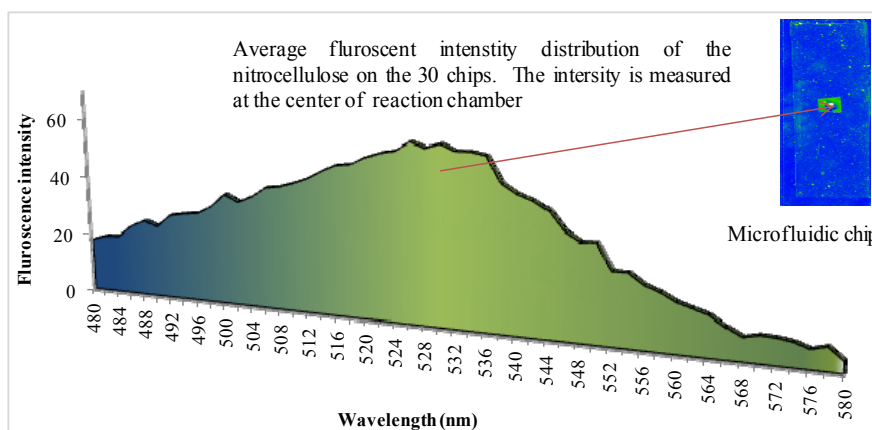


Figure 9. Average fluorescence values from the microfluidic chip.

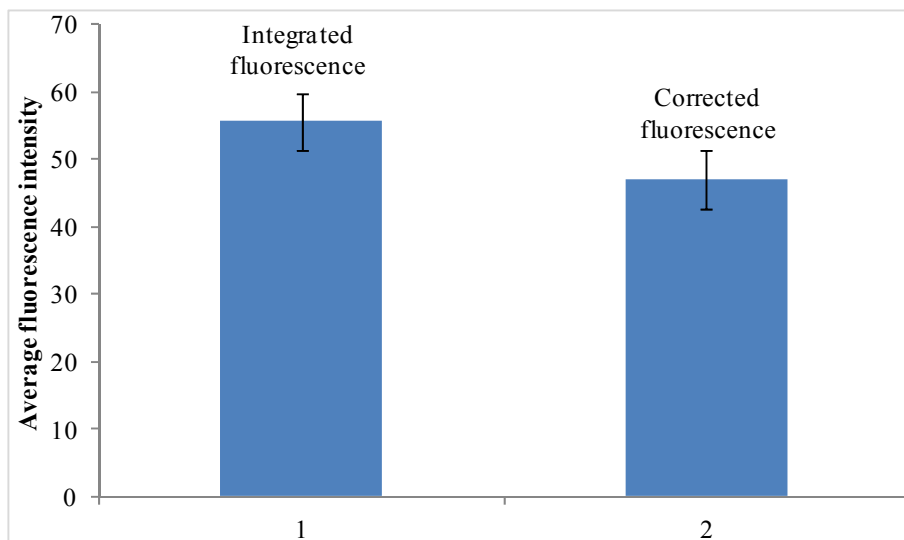
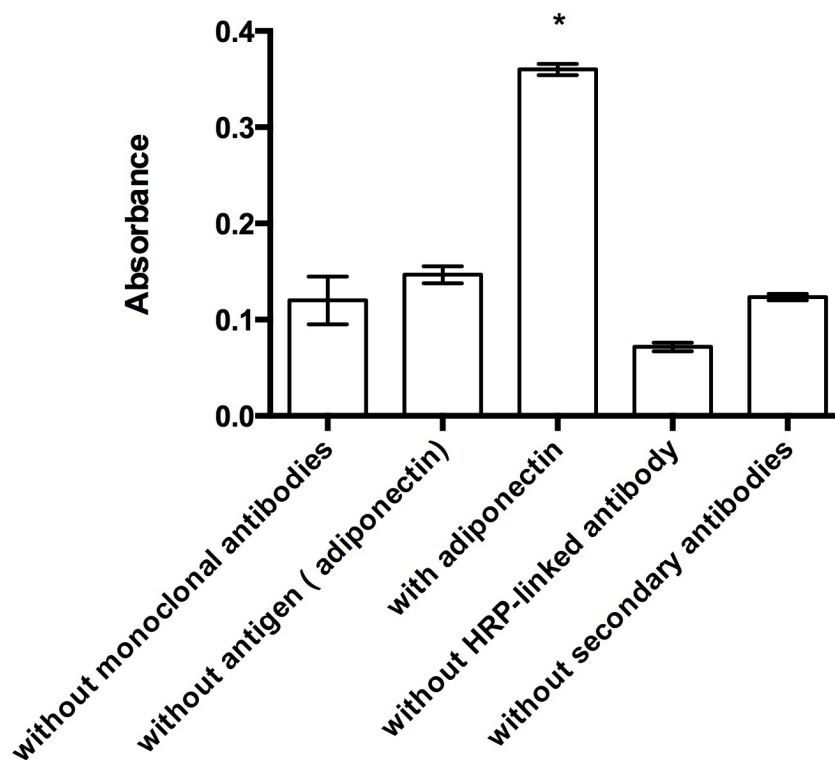


Figure 10. Controls for ELISA using fluorescence detection (one-way ANOVA analysis; “*” denotes the significant result within $p < 0.05$).



The ELISA on-chip results were also compared to conventional ELSIA off-chip results, *i.e.*, using a 96-well microtiter plate.

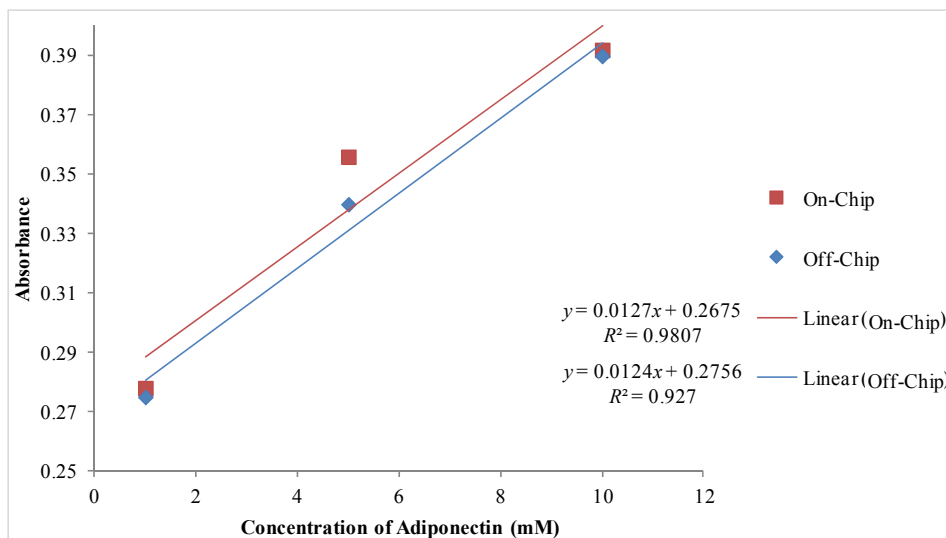
Figure 11. Analyte concentration vs. fluorescence (off-chip and on-chip).

Figure 11 shows comparative absorbance curves for different concentration of adiponectin. As the concentration of adiponectin increases, the absorbance levels also increase linearly. Higher absorbance was observed on microfluidic chip. This is attributed to the fact that microfluidic structures provide large surface area for antibody immobilization; as a result, more antigens are captured. Therefore the performing ELISA on microfluidic structure was found to be more efficient as 10%–15% higher absorbance response was observed than the one performed on 96 well micro titer plate.

Magnetic particle immunoassay was done using secondary antibody-coated magnetic beads (10-nm average size bought Taiwan Advanced Nano Beads Pvt. Lmt., Taoyuan, Taiwan) which formed the bio-complex structure as shown in Figure 1. First, the measurement of the magnetic field from the beads was done using a circuit consisting of differential pair of inductors. In Figure 12, the system shows two inductors, measuring inductor and reference electrode, with the same open-circuit voltage. It also shows the microfluidic chip integrated with it, whereby the reaction chamber sits directly on the top of one of the inductors. The load that changes the voltage is in the form of a magnetic field from beads. The response is measured as a phase shift in the voltage of a measuring inductor.

We found that there was a difference in a time period of 4 ns without any magnetic beads placed over any of the inductors. Subsequently, we placed sets of 10, 20, 40, 50, 80, 100 $\mu\text{g}/\mu\text{L}$ solution of magnetic beads on one inductor using a syringe pump. The solution consisted of magnetic beads coated with the antibody of adiponectin and the analyte with a concentration of 10 mM. The total volume of the solution was confined to 100 μL . A considerable amount of change in the phase of the signal from one of the inductors was seen. Figure 13 plots the results from the magnetic beads. It is seen that the magnetic field from the beads varies linearly with the number of beads

Figure 12. Differential pair of inductors measuring signal from magnetic beads on microfluidic platform.

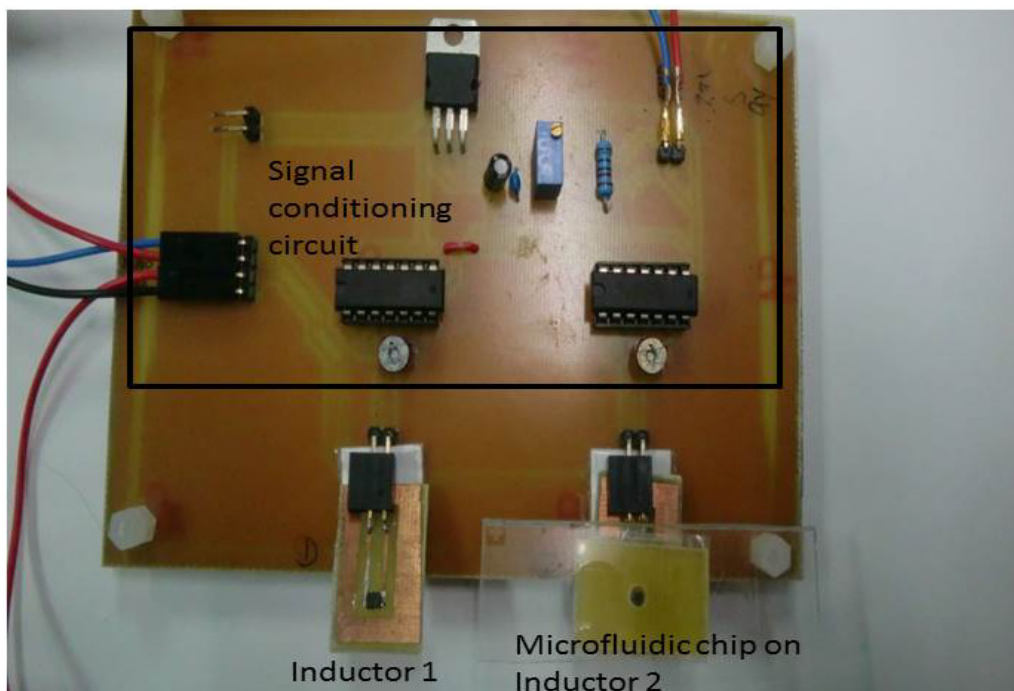
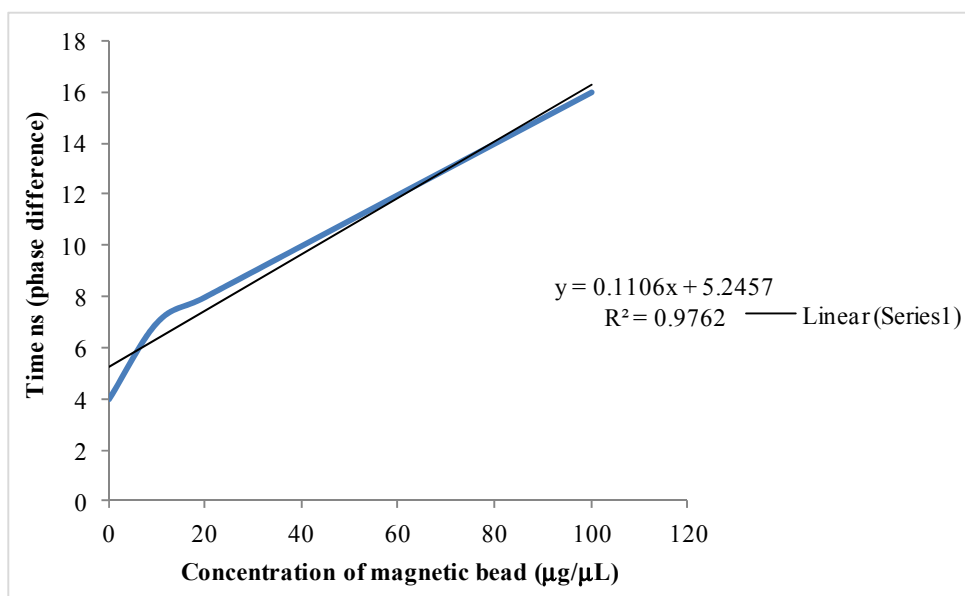


Figure 13. Graph indicating linearity of the magnetic field measurements from different sets of magnetic beads.



The final detection was done using a fabricated Hall sensor. The induction coil below the the Hall sensor is actuated with a current of 39.8 mA. This produces a magnetic field, which polarizes the magnetic beads. Since magnetic beads are composed of superparamagnetic particles, they retain a certain amount of magnetism as they experience magneto static force derived in Equation (1). This changes the total magnetic field that is sensed by the Hall sensing area. Now the Hall sensor has an effect of two super positioned magnetic field, one from the induction coil and another from the bead.

The Hall sensor is started with a current of 100 μA that is deflected by the aforementioned super-positioned magnetic field. This produces a Hall voltage of around 0.4 V for 0.01 Tesla magnetic field. The graph in Figure 14 shows the post fabrication testing result of Hall sensor (Hall’s voltage vs. magnetic field). The results show a linear curve with a regression co-efficient of 0.996. The magnetic field from the Hall sensor was measured from the ferro-fluid consisting of 10-nm superparamagnetic particles. The results match with the simulation results of COMSOL in Figure 15, which shows a Hall voltage distribution with maximum Hall voltage of 0.40 V.

Figure 14. Magnetic flux (Input) vs. voltage (Output) curve.

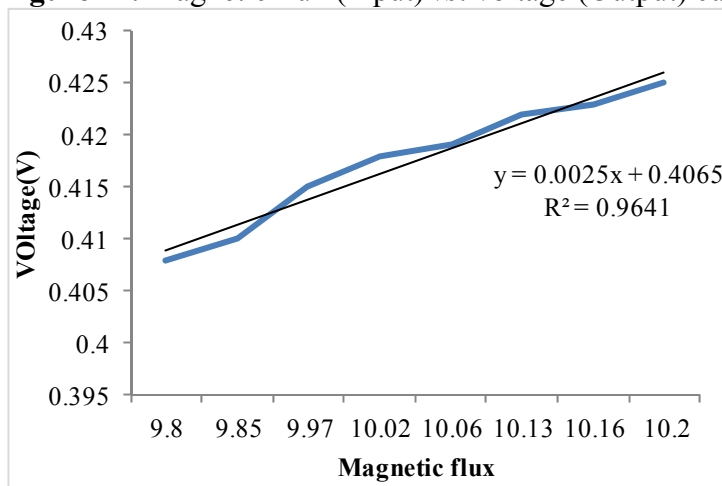
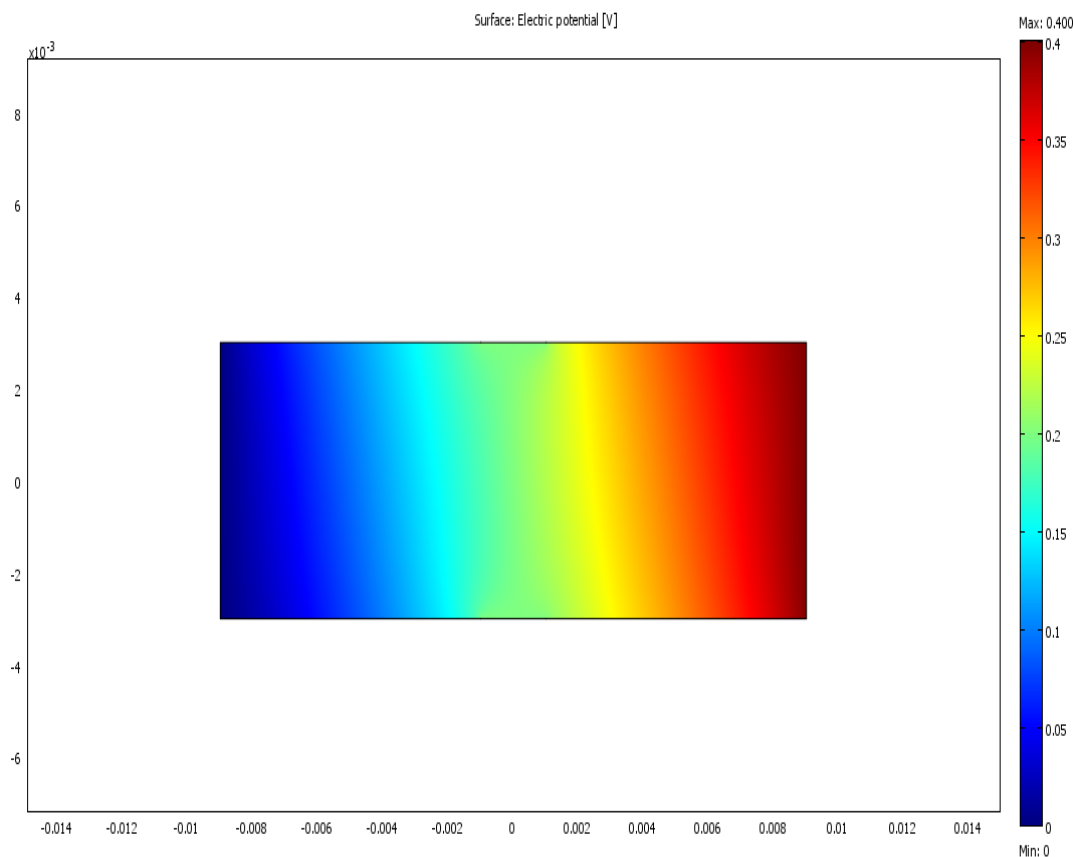


Figure 15. Top view of Hall’s voltage distribution.



4. Conclusions

We successfully demonstrated immunoassay for adiponectin on a microfluidic chip. The chip shows capability of carrying magnetic particle-based immunoassay. The microfluidic platform was constructed using PDMS and nitrocellulose. The fabricated Hall sensor formed a major part of the magnetic particle detection system. The sensor was placed below the microfluidic channel where the immunoassay reaction takes place. We observed that the distance between the magnetic bead and Hall sensor is crucial in sensing the magnetic bead since the magnetic field varies inversely to the cube of distance between the sensor and the bead. In the near future, we intend to submit a complete report on Hall sensor detection of immunoassay. This study provides a point-of-care testing solution for the immunoassay.

Acknowledgments

The authors are grateful to the National Science Council, Taiwan, R.O.C., for providing financial support to work on the project NSC-99-221-E-033-064, NSC-100-2221-E-033-051 and NSC 101-2221-E-033 -068. In addition, we also deeply appreciate the National Chip Implementation Centre, Taiwan, R.O.C., for technical support and chip fabrication.

Conflict of Interest

The authors declare they have no conflicts of interest.

References

1. Chin, C.D.; Laksanasopin, T.; Cheung, Y.K.; Steinmiller, D.; Linder, V.; Parsa, H.; Wang, J.; Moore, H.; Rouse, R.; Umviligihozo, G.; *et al.* Microfluidics-based diagnostics of infectious diseases in the developing world. *Nat. Med.* **2011**, *17*, 1015–1019.
2. Srinivasan, V.; Pamula, V.K.; Fair, R.B. Droplet-based microfluidic lab-on-a-chip for glucose detection. *Anal. Chim. Acta* **2004**, *507*, 145–150.
3. Kergaravat, S.V.; Beltramino, L.; Garnero, N.; Trotta, L.; Wagener, M.; Isabel Pividori, M.; Hernandez, S.R. Electrochemical magneto immunosensor for the detection of anti-TG2 antibody in celiac disease. *Biosens. Bioelectron.* **2013**, *48C*, 203–209.
4. Hung, L.-Y.; Chuang, Y.-H.; Kuo, H.-T.; Wang, C.-H.; Hsu, K.-F.; Chou, C.-Y.; Lee, G.-B. An integrated microfluidic platform for rapid tumor cell isolation, counting and molecular diagnosis. *Biomed. Microdevices* **2013**, *15*, 339–352.
5. Srinivasan, V.; Pamula, V.K.; Fair, R.B. An integrated digital microfluidic lab-on-a-chip for clinical diagnostics on human physiological fluids. *Lab Chip* **2004**, *4*, 310–315.
6. Yeo, L.Y.; Chang, H.-C.; Chan, P.P.Y.; Friend, J.R. Microfluidic devices for bioapplications. *Small* **2011**, *7*, 12–48.
7. Fair, R.B. Digital microfluidics: Is a true lab-on-a-chip possible? *Microfluid. Nanofluid.* **2007**, *3*, 245–281.

8. Yamauchi, T.; Kamon, J.; Waki, H.; Terauchi, Y.; Kubota, N.; Hara, K.; Mori, Y.; Ide, T.; Murakami, K.; Tsuboyama-Kasaoka, N.; *et al.* The fat-derived hormone adiponectin reverses insulin resistance associated with both lipodystrophy and obesity. *Nat. Med.* **2001**, *7*, 941–946.
9. Bruls, D.M.; Evers, T.H.; Kahlman, J.A.H.; van Lankvelt, P.J.W.; Ovsyanko, M.; Pelssers, E.G.M.; Schleipen, J.J.H.B.; de Theije, F.K.; Verschuren, C.A.; van der Wijk, T.; *et al.* Rapid integrated biosensor for multiplexed immunoassays based on actuated magnetic nanoparticles. *Lab Chip* **2009**, *9*, 3504–3510.
10. Owen, D.; Mao, W.; Alexeev, A.; Cannon, J.; Hesketh, P. Multiplexed electrochemical immunoassay of biomarkers using metal sulfide quantum dot nanolabels and trifunctionalized magnetic beads. *Micromachines* **2013**, *4*, 103–115.
11. Owen, D.; Mao, W.; Alexeev, A.; Cannon, J.; Hesketh, P. Electrochemical magneto immunosensor for the detection of anti-TG2 antibody in celiac disease. *Micromachines* **2013**, *4*, 103–115.
12. Owen, D.; Mao, W.; Alexeev, A.; Cannon, J.; Hesketh, P. Microbeads for sampling and mixing in a complex sample. *Micromachines* **2013**, *4*, 103–115.
13. Aytur, T.; Foley, J.; Anwar, M.; Boser, B.; Harris, E.; Beatty, P.R. A novel magnetic bead bioassay platform using a microchip-based sensor for infectious disease diagnosis. *J. Immunol. Methods* **2006**, *314*, 21–29.
14. Lu, M.; Zhai, H.; Magnusson, R. Focusing light with curved guided-mode resonance reflectors. *Micromachines* **2011**, *2*, 150–156.
15. Chang, A.-Y.; Lu, M.S.-C. A CMOS magnetic microbead-based capacitive biosensor array with on-chip electromagnetic manipulation. *Biosens. Bioelectron.* **2013**, *45*, 6–12.
16. Florescu, O.; Wang, K.; Au, P.; Tang, J.; Harris, E.; Beatty, P.R.; Boser, B.E. On-chip magnetic separation of superparamagnetic beads for integrated molecular analysis. *J. Appl. Phys.* **2010**, *107*, 54702, doi:10.1063/1.3272779.
17. Florescu, O.; Mattmann, M.; Boser, B. Fully integrated detection of single magnetic beads in complementary metal-oxide-semiconductor. *J. Appl. Phys.* **2008**, *103*, 046101, doi:10.1063/1.2840062.
18. Bettazzi, F.; Hamid-Asl, E.; Esposito, C.L.; Quintavalle, C.; Formisano, N.; Laschi, S.; Catuogno, S.; Iaboni, M.; Marrazza, G.; Mascini, M.; *et al.* Electrochemical detection of miRNA-222 by use of a magnetic bead-based bioassay. *Anal. Bioanal. Chem.* **2013**, *405*, 1025–1034.
19. Zhou, C.-H.; Long, Y.-M.; Qi, B.-P.; Pang, D.-W.; Zhang, Z.-L. A magnetic bead-based bienzymatic electrochemical immunosensor for determination of H9N2 avian influenza virus. *Electrochem. Commun.* **2013**, *31*, 129–132.
20. Choi, J.-W.; Oh, K.W.; Thomas, J.H.; Heineman, W.R.; Halsall, H.B.; Nevin, J.H.; Helmicki, A.J.; Henderson, H.T.; Ahn, C.H. An integrated microfluidic biochemical detection system for protein analysis with magnetic bead-based sampling capabilities. *Lab Chip* **2002**, *2*, 27–30.
21. Lin, Y.-H.; Wang, S.-H.; Wu, M.-H.; Pan, T.-M.; Lai, C.-S.; Luo, J.-D.; Chiou, C.-C. Integrating solid-state sensor and microfluidic devices for glucose, urea and creatinine detection based on enzyme-carrying alginate microbeads. *Biosens. Bioelectron.* **2013**, *43*, 328–335.

22. Zhuang, J.; Fu, L.; Xu, M.; Zhou, Q.; Chen, G.; Tang, D. DNAzyme-based magneto-controlled electronic switch for picomolar detection of lead (II) coupling with DNA-based hybridization chain reaction. *Biosens. Bioelectron.* **2013**, *45*, 52–57.
23. Lu, A.-H.; Salabas, E.L.; Schüth, F. Magnetic nanoparticles: Synthesis, protection, functionalization, and application. *Angew. Chem. Int. Ed.* **2007**, *46*, 1222–1244.

© 2013 by the authors; licensee MDPI, Basel, Switzerland. This article is an open access article distributed under the terms and conditions of the Creative Commons Attribution license (<http://creativecommons.org/licenses/by/3.0/>).